# Healing Process of Bone Defects Based on the Location of Lesion with Osteogenesis Markers and Defect Size Measurement: A Preliminary Study

Lusi Epsilawati[1]*, Azhari[1], Merry Annisa Damayanti[1], Aga Satria Nurrachman[2], Fadhlil Ulum Abdul Rahman[3], Norlaila Sarifah[4], Putri Marina Sukmadewi[5], Mahindra Awwaludin Romdlon[5]

1. Department of Dentomaxillofacial Radiology, Faculty of Dentistry, Universitas Padjadjaran, Bandung, West Java, Indonesia.
2. Department of Oral and Maxillofacial Radiology, Faculty of Dental Medicine, Universitas Airlangga, Surabaya, Indonesia.
3. Department of Oral and Maxillofacial Radiology, Faculty of Dentistry, Hasanuddin University, Makassar, Indonesia.
4. Department of Dentomaxillofacial Radiology, Faculty of Dentistry, Lambung Mangkurat University, Banjarmasin, Indonesia.
5. Resident of Dentomaxillofacial Radiology Specialist Program, Faculty of Dentistry, Universitas Padjadjaran, Bandung, West Java, Indonesia .

**Abstract**

The bone defect, characterized by the undesired loss of bone material, can arise from post-infection cavities, lesion therapy, or fractures, presenting a complex and challenging healing process. This condition is influenced by various contributing factors. Long bones are categorized into three segments (epiphysis, metaphysis, and diaphysis) under the Universal Long Bone Defect Classification.

This study aimed to determine differences in the healing process of bone defects based on the position of the defect. Conducted on 60 male Wistar rats (12 weeks old, weighing 250-300 mg), the experiment includes two groups: Group A (30 animals with metaphyseal defects) and Group B (30 animals with diaphyseal defects). Each group was divided into smaller subgroups, each consisting of 6 animals, based on designated observation days: H0, 5, 10, 17, and 25. This arrangement led to the formation of ten groups in total.

The assessment involves osteogenesis markers and defect area measurement from radiographs, revealing higher values for osteoblasts and osteoclasts in Group B, except for Group A chondrocytes which exhibit higher values. Additionally, the lesion area in Group B is smaller. Statistical analysis confirms these differences, leading to the conclusion that bone defects in the diaphyseal area exhibit faster healing compared to the epiphyseal or metaphyseal regions.

**Experimental article (J Int Dent Med Res 2024; 17(1): 161-167)**

**Keywords:** Bone Defect, Epiphysis, Diaphysis, Metaphysis, Location of Defect.

**Received date:** 26 December 2023 **Accept date:** 26 January 2024

## Introduction

A bone defect is a condition where part of the bone is lost due to trauma or infection. In dental tissue, bone defects often occur in the alveolar bone, with infections caused by periodontal disease.[1,2,3] According to Goldman et al.'s classification, alveolar bone defects are divided into intrabony defects and craters. Intrabony defects have been classified according to their structure based on the remaining bony wall, the defect's width, and its topographic extent around the tooth. Another classification often used is the classification according to Hamp et al., which determines the classification based on tooth furcation involvement.[4-7] Unlike the classification of long bones, the Universal Long Bone Defect Classification (ULBDC) has determined the classification of bone defects, which divides bone defects based on the lesion's location and shape. The location of the lesion referred to in the long bones is segment one, which is located in the epiphysis area (proximal area of the bone), segment two, which is located in the metaphysis area (middle of the bone) and segment three which is in the diaphysis area or distal periarticular area of the bone.[8,9]

In the healing process of bone defects, the long bones and the jaw proceed through the same process, although there are slight

*Corresponding author:
Lusi Epsilawati,
Department of Dentomaxillofacial Radiology,
Faculty of Dentistry, Universitas Padjadjaran,
Bandung, Indonesia
E-mail : lusi.epsilawati@fkg.unpad.ac.id

differences in the proliferation phase. In principle, the recuperation of bone defects follows the same intricate and challenging process as general bone healing. This complexity arises from the involvement of numerous factors, leading to overlapping healing phases.[9,10]

Studies that assess how the healing process of bone defects in long bones with different locations differs have not been widely discussed. This study was designed to assess possible differences in markers of osteogenesis, specifically osteoblasts, osteoclasts, and chondrocytes, as well as the size of defects in radiographic images.

## Materials and methods

*Surgical and Radiographic Standards*

This experimental research was carried out at the Veterinary Teaching Hospital Institut Pertanian Bogor (RSHP IPB) and the research protocol received approval from the Animal Ethics Committee, Faculty of Veterinary Medicine, Bogor Agricultural University, Indonesia (Reference number 023/KEH/SKE/XII/2020). This research was conducted for six months, from February 2021 to June 2022. The population of this research was male Wistar rats (*Rattus Novergicus*), 12 weeks old, with a body weight of 250-300 mg. The samples utilized in this study were determined using Ferderer's formula, with a 10% correction applied if there were instances of experimental animal mortality during the study period. As a result, the total sample size for this study comprised 60 mice. Prior to the research, the mice underwent a two-week adaptation period, during which their food, drink, and maintenance adhered to hospital standards. Additionally, they received worm medicine and vitamins. The surgical procedure commenced with the weighing of all mice, followed by the shaving of hair on the right leg. Subsequently, mice were anesthetized with doses adjusted based on their body weight. Anesthesia was carried out with a combination of 10 mg ketamine hydrochloride (Pharmamadix Corp, Peru) and 3 mg xylazine hydrochloride (Interchemie werken “De Adelaar” BV, Venray, Holland) intramuscularly. An incision is made in the right femur until the bone surface is visible. Then, a box-shaped defect is made with a rounded bottom edge measuring 4x4 until the bone is penetrated towards the back. Drilling using a diamond drill in the form of a short fissure, 1 cm long and 4 mm in diameter, was carried out under the control of spooling sterile distilled water. Finally, trim the edges of the bone so that there are no sharp edges of the defect wall. Thirty bone defects were made in the diaphysis with a distance of 1 cm from the neck of the head (after this, referred to as group A), and 30 defects were made in the diaphysis area around the middle of the femur bone after this referred to as group B, seen in Figure 1. The wound was then sutured, part of the muscles with 4.0 vicryl thread and the skin with 3.0 silk thread. After that, an x-ray was carried out using an Indoray branded x-ray machine, type IKL-17E-100/24. The machine's serial number is BL-613238-ME, and its power is 24 Volt, DC 50 Hz, 5Amp, and it was produced by PT. Poly Jaya Medical. X-ray is carried out with settings Kv 40, mA 30, and time 0.10 seconds. Try keeping the animal in the centre of the X-ray table with the distance indicator from the table to the end of the tube 90 cm. Mice were divided into five groups based on days of observation, namely D0, 5, 10, 17, and 25, each group numbering six animals/group. After all the procedures were carried out, the animals were returned to the cage and given the antibiotic Amoxicillin Long Acting 15 mg/kgBW (IM) and the analgesic Flunixn 2.5 mg/kgBW by IM, except for 12 animals which were included in the D0 group, either group A or class B. Animals included in group D0, after all animals have been x-rayed, the euthanasia procedure is carried out by injecting another anaesthetic with an overdose of around 40 mg/kg ketamine hydrochloride (Pharmamadix Corp, Peru) and 10 mg/kg xylazine hydrochloride (Interchemie werken“De Adelaar” BV, Venray, Holland) intramuscularly. The animal was then necropsied to take part of the femur and put in a tube that had been labelled and filled with 10% Normal Buffer Formalin (BNF). The remaining waste is reported to the hospital for subsequent destruction according to the standards used in animal hospitals for processing in the incinerator section. On the following day, on D5, all animals were taken out of the cage, and their body weights were weighed. They were then anaesthetized, followed by an X-ray examination. For the 12 animals on D5, euthanized was performed using the same procedure as in the previous group; the femur from the necropsy was placed in a tube that had been labelled and 10% BNF. This

procedure was implemented up to D25 on all euthanized animals (total of 60), resulting in the collection of 60 femur samples.

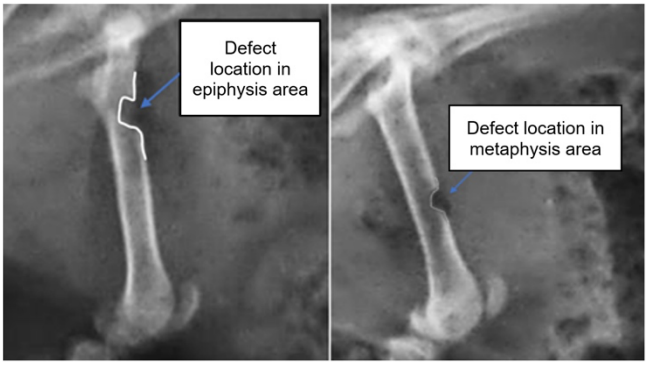


**Figure 1.** Creation of defects in the epiphysis and diaphysis regions of the femur bone, each measuring approximately 4 mm in diameter.


**Figure 2.** Research procedures, a. Mice with the same diets and drink droplets, b. Ketamine anesthesia, c. Xylostesin injection, d. Anaesthetic injection procedure, e. Creating an incision and hole to locate the femur bone.

*Procedure for making HPA analysis*

Sixty femur samples were soaked in a 10% BMF solution, and the preparation process commenced with a dehydration step. The samples were subsequently immersed in alcohol with varying concentrations (80%, 85%, 90%, and 95%), each for a duration of 2 hours. The final immersion lasted for 12 hours.[11,12] The procedure was then continued by making preparations to observe the osteoblast and osteoclast cells, stained with hematoxylin-eosin, while chondrocyte cells were stained with Masson's trichome.[11,12] The number of preparations was adjusted to match the initial sample count, with 5 preparations for each group. Consequently, 60 preparations were made across the 10 groups (Figure 3).

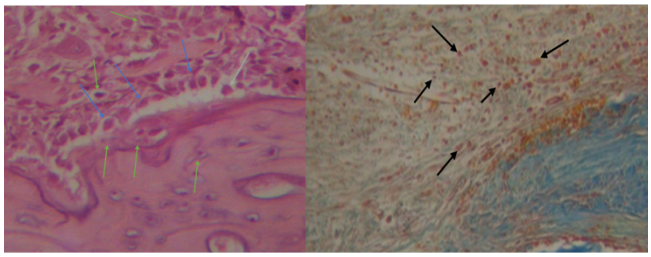

**Figure 3.** The histopathological image of the sample showing osteoblast cells (blue arrow), osteoclast (green arrow), and chondrocyte cells (black arrow).

*Radiographic Analysis*

The radiographic analysis that is calculated is the area of the defect area on the radiograph. Measurements were carried out using rearrangement measurements on ImageJ software. The procedure involves selecting the radiograph for measurement, zooming in until the image is clear, initiating the measurement with the rectangular feature, recording the measurement, and generating the results.[13]

*Statistical Analysis*

Statistical analysis was performed using SPSS version 18 software (SPSS, Chicago, Illinois, USA). The results are presented in a table containing mean, median, SD, ρ, and sig. (2-tailed). Differential tests were carried out between all variables, namely osteoblasts, osteoclasts, chondrocytes, and the size of the defect area. Measurement is carried out by counting the number of cells visible on the microscope; the software imageJ cell counter feature assists in the calculation and calculates the defect area using the rectangular feature. Before carrying out calculations, it is necessary to carry out a normality test. In this study, the Shapiro-Wilk test was employed due to the small dataset, with the criterion that ρ>0.05 is considered normal. Then, the independent sample T-Test was conducted, indicating a significant difference if the sig value. (2-tailed) is greater than 0.05.

## Results

This study compares the healing process of bone defects in the epiphysis and diaphysis

areas. The research was carried out in two groups, each observed for five days, resulting in a total of 10 data points. The distribution of the data was initially assessed, revealing that the average of the 10 data points exhibited a non-normal distribution (ρ<0.05), whereas the data could be said to be normal if it had ρ>0.05. Notably, the osteoblast data for group A and the osteoclast data for both groups A and B demonstrated normally distributed patterns (Table 1).

| | Mean | Median | Sd | ρ |
|---|---|---|---|---|
| Collagen | | | | |
| A | 23.022 | 27.114 | 9.98 | 0.014 |
| B | 24.201 | 26.194 | 9.947 | 0.014 |
| Osteoblast | | | | |
| A | 2463.6 | 2459 | 848.27 | 0.246 |
| B | 2499,6 | 2380 | 937.05 | 0.03 |
| Osteoclast | | | | |
| A | 22.5 | 22.47 | 6.886 | 0.502 |
| B | 24.36 | 25 | 27 | 0.347 |
| Size of Defect Area | | | | |
| A | 11.64 | 8 | 10.4 | 0.001 |
| B | 10 | 8 | 15.55 | 0.001 |

**Table 1.** Description of data from groups A and B.

| | D0 | D5 | D10 | D17 | D25 |
|---|---|---|---|---|---|
| Collagen | | | | | |
| A | 7 | 17.78 | 28.28 | 33.57 | 28.46 |
| B | 7.8 | 22.16 | 30.77 | 35.66 | 24.63 |
| Sig. (2-tailed) | 0.147 | 0.075 | 0.161 | 0.182 | 0.084 |
| Osteoclast | | | | | |
| A | 18.8 | 25 | 32.2 | 21.2 | 15.2 |
| B | 18.6 | 26 | 35.4 | 27.2 | 14.6 |
| Sig. (2-tailed) | 0.958 | 0.825 | 0.033 | 0.006 | 0.766 |
| Osteoblast | | | | | |
| A | 1658.2 | 1648.6 | 2566.6 | 2830.2 | 3614.4 |
| B | 1335 | 1753.8 | 2409.8 | 3290.8 | 3708.6 |
| Sig. (2-tailed) | 0.286 | 0.727 | 0.298 | 0.17 | 0.412 |
| Size of Defect Area | | | | | |
| A | 28 | 12.6 | 7.8 | 6.6 | 2.8 |
| B | 27 | 12.6 | 7.2 | 3.2 | 2.2 |
| Sig. (2-tailed) | 0.912 | 1 | 0.766 | 0.163 | 0.447 |

**Table 2.** The t-test results.

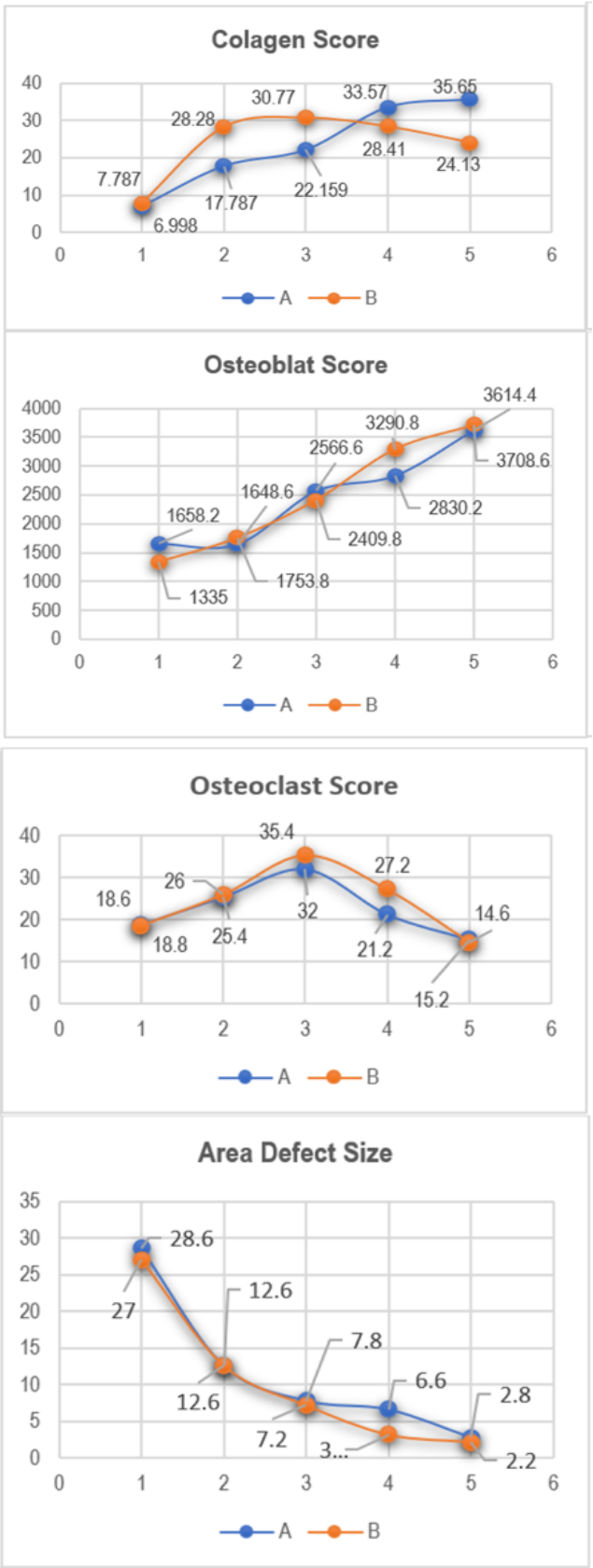


**Figure 4.** Graphical pattern of chondrocyte, osteoblast, osteoclast values, and the size of the defect area.

Moreover, the average values of all groups are depicted in Figure 4. The graphical representation shows a significantly higher chondrocyte value in group B compared to group A. It can also be seen that the chondrocyte value in group B peaks at D10 and then immediately decreases, aligning with the decline in the proliferation phase of the process. The graphical pattern is nearly identical in depicting osteoblasts, osteoclasts, and the defect area. Both of them seem to co-occur and show minimal distinctions.

After carrying out a difference test between groups using the t-test, it can be seen that all the data in both groups exhibit significant differences, with only two data that are not significant, specifically the osteoblast values at D10 and 17 (Table 2). It showed that the data in group B showed a faster healing rate compared with data in group A.

## Discussion

The healing process for bone defects is intricate and challenging, particularly when comparing the healing mechanisms in the epiphysis/metaphysis and diaphysis regions—a distinction we seek to elucidate. Initially, we categorized bones into segments following the Universal Long Bone Defect Classification (ULBDC), comprising epiphysis, metaphysis, and diaphysis. The epiphysis, situated at the end of a long bone, contributes to growth. The epiphyseal growth plate, positioned between the shaft and epiphysis, facilitates cartilage proliferation, leading to bone elongation. Metaphysis encompasses the region below the epiphysis, extending from the neck area of the joint to approximately 2-3 cm towards the middle of the bone. The diaphysis, located centrally in the bone, is characterized by thick cortical bone and dense trabeculae. Progressing from the exterior to the interior, the layers of the diaphysis are initially enveloped by the periosteum, followed by trabeculae and endosteum towards the interior.[14-16]

Physiologically, bone formation can be divided into two ways, namely endochondral and intramembranous growth.[14-16] In the defect healing process, endochondral growth dominates the growth. Closure of the defect begins with the growth of chondrocytes, which are then replaced by mineralized osteocytes. Osteocytes themselves are produced from osteoblast cells. The osteoclast provides the space where bones are formed through the resorption of chondrocyte tissue composed of collagen cells.[14] All these processes can be achieved perfectly with an adequate blood supply, starting from forming fibrous tissue, which is then replaced by collagen. Ultimately, the progression involves the replacement of collagen with bone tissue, beginning as a soft callus and transitioning into a hard callus.[17]

The epiphysis and metaphysis areas are physiologically closer to the growth center and to the body plate in the joint head area. This area is dominated by chondrocyte tissue. Calcification in this area is greatly influenced by movement and the need for bones to grow in length. This makes the bones in this area tend to be brittle, and if the injury occurs at a growing age, the child's growth and development will be disrupted.[18]

Based on the research results, it can be seen that the healing process of defects in the epiphysis/metaphysis area is slower than in the diaphysis area. This can be seen from the number of cells, including chondrocytes, osteoblasts, and osteoclasts, less than the defects in the diaphysis area. This delay can also be seen from the value of the defect area, where the defect area shrinks faster in group B compared to group A. This observation aligns with findings in studies conducted by Cepela et al.[18] and Belt et al.[19].

Based on the location of bone fractures and defects in the epiphysis area, Salter and Harris (1963) divided them into five conditions: five types. These five types are: type I is an injury that divides the epiphysis area into upper and lower parts, type II is an injury that covers the middle area of the epiphysis and extends to the metaphysis with an oblique shape, type III injury is located from the base of the epiphysis to the middle of the epiphysis, type IV is a shaped injury that covers the epiphysis and metaphysis area and type V is a comminuted fracture in the epiphysis area.[18,20] Locations or formations that are not included in the classification of Salter and Harris, agreed by Peterson and Burkhart, will be classified based on the condition and etiology, this is supported by Rathjen and Birch.[17,20,21,22]

Based on the Salter and Harris classification, the defect created is included in the type IV classification, where the defect is created in the metaphysis area. This area is said to be an area of calcification, and it is said to be

so because there are many chondrocyte cells and calcification of osteocytes that occur in type IV. Salter and Harris also explained that the epiphysis area contains many chondrocyte cells, where the closer to the diaphysis, the chondrocytes become more mature and active. In contrast, the area towards the epiphysis is said to be the proliferation zone and hypertrophic zone. In the calcification zone, there are also osteoblast and osteoclast cells.[19,20] Salter and Harris also reported that most of the blood supply in the epiphysis is obtained from the surrounding periosteum layer. Meanwhile, the calcification zone is a zone that is outside the epiphysis area so that the area is prone to blood supply. The blood supply in this area is thought to come from the flow of blood vessels in the periosteum, which runs from the side of the bone.[19,20] This condition explains why the healing process of defects in the area The epiphysis and metaphysis progress more slowly compared to defects located in the diaphysis area.

Conditions in the diaphysis area significantly differ from those in the epiphysis and metaphysis areas. In the diaphysis, osteoblasts and osteocytes are commonly present, along with osteoclasts, whereas chondrocytes are infrequently found. Blood supply in this region is provided by the Haversian vessels, which are abundant in blood vessels. The diaphysis undergoes frequent remodeling, ensuring continuous growth and development in the lateral area, encompassing both endochondral and intramembranous processes.[22]

## Conclusions

The healing process of bone defects in the epiphysis and metaphysis regions takes longer compared to the diaphysis area. This is supported by the higher count of osteoblast and osteoclast cells in the diaphysis region, whereas chondrocytes are more abundant in the epiphysis area.

## Acknowledgements

This research received financial support from the Rector's Assistance Fund, Padjadjaran University, Bandung, West Java, Indonesia. Additional support was provided by the Faculty of Dentistry and Faculty of Medicine, Universitas Padjadjaran, Bandung, West Java, Indonesia. The authors extend their gratitude to the Biotech Chemistry Lab at Padjadjaran University, Eyckman Unpad Laboratory, and Pusdi Dental Materials for their assistance in the research process, including providing tools and permits. The authors would also like to thank the Faculty of Veterinary Medicine and the personnel of the Veterinary Teaching Hospital Institut Pertanian Bogor (RSHP IPB), Bogor, West Java, Indonesia, for their valuable contributions to the research.

All authors have made substantive contributions to this study and manuscript, and all have reviewed the final paper before its submission.

## Declaration of Interest

The authors report no conflict of interest.

## References

1. Schemitsch EH. Size Matters: Defining Critical in Bone Defect Size. *Journal Orthop Trauma*. 2017;31 Suppl 5:20–2.
2. Tsuchida S, Nakayama T. Recent Clinical Treatment and Basic. Research on the Alveolar Bone. Biomedicines. 2023;11(3):843.
3. Fitriananda AK, Kiswanjaya B, Bachtiar-Iskandar HH. Alveolar Bone Loss Analysis on Dental Digital Radiography Image. Makara J Health Res. 2021:25(2):122-7.
4. Hasegawa Y, Takayama T, Iwano Y. Clinical classification of tooth position in the alveolar bone housing with periodontal defects. Journal of Dental Sciences. 2021;16(2):795-8.
5. Goldman HM, Cohen WD. The infra bony pocket: classification and treatment. J Periodontol.1958;29:272e91.
6. Hamp SE, Nyman S, Lindhe J. Periodontal treatment of multirooted teeth. Results after five years. J Clin Periodontol. 1975;2:126e35.
7. Ozcan G, Sekerci AE. Classification of alveolar bone destruction patterns on maxillary molars using cone-beam computed tomography. Niger J Clin Pract. 2017;20:1010-9.
8. Solomin L, Komarov A,Semenistyy A, Sheridan GA, Rozbruch SR. Universal long bone defect classification. J Limb Lengthen Reconstr. 2022;8:54-62.
9. Morgan EF, De Giacomo A, Gerstenfeld LC. Overview of Fracture Healing and Its Assessment. *Methods Mol Biol*. 2014;1130:13–31.
10. Einhorn TA, Gerstenfeld LC. Fracture healing: mechanisms and interventions. *Nat Rev Rheumatol Journal*. 2015;11(1):45-54.
11. Robika, Anggraeni, Irwanto R. Pelatihan Pembuatan Preparat Biologi Sebagai Sarana Peningkatan Media Pembelajaran Bagi Guru-Guru Biologi Di Kabupaten Bangka. J-Abdi Jurnal Pengabdian Kepada Masyarakat. 2023;2(11):6-12.
12. Berata IK. Teknik Pembuatan Preparat Histopotologi. Repository Universitas Udayana Bali. 2018. Available at: https://erepo.unud.ac.id/id/eprint/21511. Accessed December 30, 2022.
13. Schneider CA, Rasband WS, Eliceiri KW. NIH Image to ImageJ: 25 years of image analysis. Nat Methods. 2012 Jul;9(7):671-5.
14. Setiawati R, Rahardjo P. Bone Development and Growth. *IntechOpen*. 2019:1-21.
15. Vanputte CL, Regan JL, Russo AF. Skeletal system: Bones and joints. In: Seeley's Essentials of Anatomy & Physiology. 8th ed. USA: McGraw Hill; 2013:110-49.
16. Muscolino JE. Kinesiology the Skeletal System and Muscle Function. 2nd ed. New York: Elsevier Inc.; 2011.

17. Murshed M. Mechanism of Bone Mineralization. *Cold Spring Harb Perspect Med*. 2018;8(12):1-11.
18. Cepela DJ, Tartaglione JP,Dooley TP, Patel PN. Classifications In Brief: Salter-Harris Classification of Pediatric Physeal Fractures. Clin Orthop Relat Res. 2016 Nov;474(11):2531-7.
19. Belt M, Smulders K, Van Houten A, Wymenga A, Heesterbeek P, van Hellemondt. What Is the Reliability of a New Classification for Bone Defects in Revision TKA Based on Preoperative Radiographs?. Clin Orthop Relat Res.2020;478:2057-64.
20. Salter RB, Harris WR. Injuries involving the epiphyseal plate. J Bone Joint Surg Am. 1963;45:587–622.
21. Peterson HA, Burkhart SS. Compression injury of the epiphyseal growth plate: fact or fiction?. J Pediatr Orthop.1981;1:377-84.
22. Rathjen KE, Birch JG. Physical injuries and growth disturbances. In: Beaty JH, Kasser JR, eds. Rockwood and Wilkins' Fractures in Children. 7th ed. Philadelphia, PA: Lippincott Williams & Wilkins; 2010:91–119.